Pergamon

Int. J. Heat Mass Transfer. Vol. 37, No. 7, pp. 1143–1153, 1994

0017-9310/94 $6.00 + 0.00

0017-9310(93)E0036-G

Critical heat flux in upflow convective boiling of refrigerant binary mixtures

G. P. CELATA, M. CUMO and T. SETARO
ENEA, Rome, Italy

(*Received* 13 *May* 1993 *and in final form* 25 *October* 1993)

Abstract—The critical heat flux (CHF) in forced convective upflow has been investigated at different compositions of the binary mixture chosen, namely R12 (CCl_2F_2) and R114 ($C_2Cl_2F_4$). The test section used consists of a vertical stainless steel uniformly heated tube, 2.1 m long, 7.57 mm ID. The experimental results show an almost linear dependence of the CHF on the composition of the mixture even though deviations from linearity have been detected as a function of thermal hydraulic conditions. A further evaluation of the boiling crisis mechanisms and their relation with the CHF has been performed. A link between boiling crisis mechanisms and the functional dependence of the CHF on the mixture composition has been found. Finally, a comparison of experimental data with available correlations is accomplished.

INTRODUCTION

THE RESEARCH on binary mixtures has not yet been conducted in an exhaustive way, particularly referring to CHF in forced flow. Existing experimental studies [1–6] on CHF in forced flow with binary mixtures are mainly related to exit low quality conditions, as reported by Collier [7] and do not include refrigerant binary mixtures. A non-linear behaviour of CHF for both non-azeotropic mixtures and azeotropic mixtures was observed in refs. [1–6]. Only at the azeotropic point do the CHF data lie on the linear line between the pure fluids. Recently, Auracher and Marroquin [8] measured the CHF for a R13B1/R114 mixture flowing in a vertical stainless steel tube electrically heated with a temperature controlled system. The authors claims that their experimental results have an almost linear behaviour of CHF with the mixture composition. Thus, apparently contradictory results have been reported on non-azeotropic mixture CHF concerning its dependence on the mixture composition. Finally, very few data are available on dryout with mixtures in upward annular flow. The present study focused on the CHF connected to the annular flow regime to evaluate the relationship between the mixture composition and the onset of boiling crisis.

EXPERIMENTAL APPARATUS

The experimental loop, schematically represented in Fig. 1, consists mainly of a piston pump, an electric heater, a condenser and a liquid tank. The maximum operating pressure of the loop is 3.5 MPa, while the maximum specific flow rate is 1800 kg m^{-2} s^{-1}; the available electrical power (DC) is 10 kW for the electric heater and 15 kW for the test section. The test section is an industrial stainless steel (AISI 316), circular duct uniformly heated (Joule effect) over a length of 2100 mm, with an inner diameter of 7.57 mm and a wall thickness of 0.975 mm. The inner surface of the tube is characterized by a cavity density of about 3.5×10^9 cavities m^{-2}, with a cavity density of 2.2×10^9 cavities m^{-2} for the size below 0.5 μm. The cavity density has been evaluated using a Digital Image Measurement System connected to an electronic microscope. The Digital Image Measurement System evaluates the number of cavities present into the inner surface of a tube sample and calculates the equivalent mouth diameter of each cavity. A typical electron micrograph of the inner surface of the test section is shown in Fig. 2: the cavities are the black spots and the scale is 1 cm : 0.5 μm. Test section instrumentation consists of 0.5 mm, K-Type insulated thermocouples distributed according to the scheme of Fig. 3 for the wall (one) and the fluid (seven) temperature measurements. Two pressure transducers measure the pressure at the inlet and outlet of the test section. A turbine flow meter measures the volumetric flow rate at the inlet of the test section. The heating power has been gauged with a watt meter. Instruments accuracy is listed in Table 1. The fluid flow is upwards, with subcooled inlet conditions. The system was charged with the mixture of R12 and R114 at the required composition by introducing known masses of each refrigerant into the storage tank. Before introducing the fluid in the experimental loop, vacuum up to 0.1 Pa has been obtained using a vacuum pump. After the fluid is introduced, the pressure inside the loop

NOMENCLATURE

C	specific heat [kJ kg^{-1} K^{-1}]
G	mass flux [kg m^{-2} s^{-1}]
i	enthalpy [kJ kg^{-1}]
Δi	latent heat of vaporization [kJ kg^{-1}]
k	equilibrium constant defined in equation (9)
K	thermal conductivity [W m^{-1} K^{-1}]
L	length [m]
M	molecular weight
p	pressure [MPa]
q''	heat flux [kW m^{-2}]
R	radius [m]
Re	Reynolds number, $uD\rho/\mu$
T	temperature [K]
X	quality
x	liquid mole fraction of the more volatile component
x_M	liquid composition based on mass of the more volatile component
y	vapour mole fraction of the more volatile component
y_M	vapour composition based on mass of the more volatile component.

Greek symbols

λ	molar fraction of liquid, defined in equation (9)
μ	dynamic viscosity [kg m^{-1} s^{-1}]
ρ	density [kg m^{-3}]
σ	surface tension [N m^{-1}]
χ	parameter defined in equation (14).

Subscripts

1	pertains to the more volatile component
2	pertains to the less volatile component
bulk	pertains to the bulk fluid
CHF	pertains to the critical heat flux condition
E	additional
i	ideal
in	inlet
L	pertains to the liquid phase
mix	pertains to the mixture
sat	pertains to saturation conditions
sub	subcooled
V	pertains to the vapour phase
w	wall
z	axial coordinate.

always exceeds the atmospheric pressure, not allowing any air re-entrance. Data acquisition is accomplished by a Macintosh Computer.

PHYSICAL PROPERTIES EVALUATION

Regarding the analysis of the data and comparison with the predictive methods, all thermodynamics properties, such as density, composition, enthalpy and saturation temperature, for both pure and mixed refrigerants were calculated by the Carnahan–Starling–DeSantis (CSD) equation of state, as proposed by Morrison and McLinden [9]. The ability of the CSD equation of state in predicting the p–v–t behaviour of R12 and R114 is shown in Table 2, where the RMS errors of the equation of state in representing the ASHRAE data [10] of saturation pressure, saturated liquid and vapour volume and enthalpy of vaporization of the two pure fluids are listed. The CSD equation of state also reproduces very well the temperature–composition diagram of the R12/R114 mixture as shown in Fig. 4 (continuous line), where the

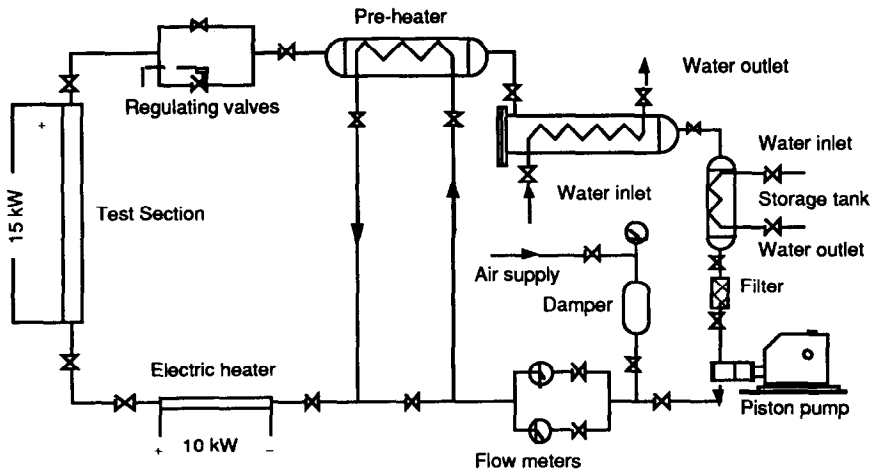

FIG. 1. Schematic of the experimental loop.

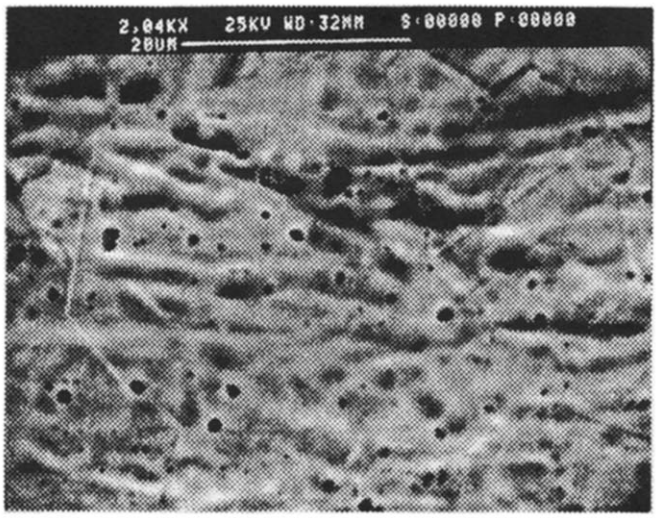

FIG. 2. Electron micrograph of the inner surface of the test section: scale 1 cm : 0.5 μm

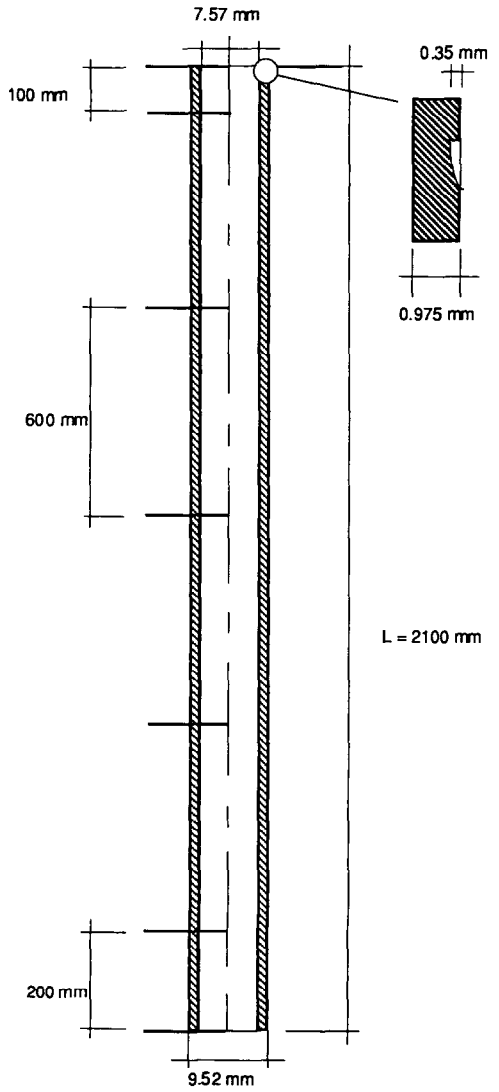

FIG. 3. Schematic of the test section.

experimental bubble point curve is represented with closed symbols and the experimental dew point curve with empty symbols.

Liquid thermal conductivity, $K_{L,mix}$, is evaluated using the correlation proposed by Filippov [11]:

$$K_{L,mix} = x_M K_{L,1} + (1-x_M)K_{L,2} - 0.72x_M(1-x_M)(K_{L,2}-K_{L,1}) \quad (1)$$

where x_M is the liquid mole-fraction based on the mass of the more volatile component, while subscripts 1 and 2 refer to the more and the less volatile components, respectively. It should be noted that the components were chosen so that $K_{L,2} \geqslant K_{L,1}$.

The liquid viscosity, $\mu_{L,mix}$, is derived with the method proposed by Kandlikar *et al.* [12]:

$$\ln(\mu_{L,mix}) = x\ln(\mu_{L,1}) + (1-x)\ln(\mu_{L,2}). \quad (2)$$

Actually, Kandlikar *et al.* [12] used the mass fraction in equation (2) in place of the mole fraction. However, it was found that the mole fraction fitted the data more closely. Thus, the mole fraction was used in the present study.

The vapour viscosity, $\mu_{V,mix}$, was obtained from the Wilke's correlation [13], given by

$$\mu_{V,mix} = \frac{y_1\mu_{V,1}}{y_1+y_2P_{12}} + \frac{y_2\mu_{V,2}}{y_2+{}_1P_{21}} \quad (3)$$

where P_{ij} is defined as

$$P_{ij} = \frac{[1+(\mu_{V,i}/\mu_{V,j})^{0.5}(M_iM_j)^{0.25}]^2}{[8(1+M_i/M_j)]^{0.5}} \quad (4)$$

and M is the molecular weight.

The surface tension of the mixture, σ_{mix}, is calculated using a linear mole fraction weighting method [14]:

$$\sigma_{mix} = x\sigma_1 + (1-x)\sigma^2. \quad (5)$$

Table 1. Instruments and their accuracy

Parameter	Instrument	Accuracy
Heating power	Wattmeter	±0.3 W
Flow rate	Turbine flow meter	$\pm 4.2 \times 10^{-8}$ m^3 s^{-1}
Temperature	K-Type insulated	±0.1 K
Pressure	Sealed strain-gauge	±4 KPa

Specific heat of liquid is calculated using a linear mass fraction weighting method [14]:

$$C_{p_{L,mix}} = x_M C_{p_{L,1}} + (1 - x_M) C_{p_{L,2}}. \quad (6)$$

LOCAL QUALITY AND LIQUID MOLE FRACTION EVALUATION

The fluid always entered the test section under subcooled conditions. Then, assuming thermodynamic equilibrium, the quality at location z, X_z, follows from an energy balance:

$$X_z = \frac{i(z) - i_{L,sat}(z)}{\Delta i(z)} \quad (7)$$

where the properties are dependent on the local liquid mole fraction of the low boiling component (R12), x_z, and the local pressure, p_z. The local pressure can be directly measured; on the contrary, the local liquid mole fraction direct measurement disturbs the fluid flow and thus should be avoided. A reasonable evaluation is however possible if a closed system evaporation and thermodynamic equilibrium at each location z is assumed, as suggested by Auracher and Marroquin [8]. The authors based this procedure on ref. [15]. This model yields x_z according to

$$x_z = \frac{x_1}{k(1-\lambda) + \lambda} \quad (8)$$

where the equilibrium constant, k, and the molar fraction of liquid, λ, are defined as

$$k = \frac{y_z}{x_z} \quad \lambda = \frac{1 - X}{1 + X(M_L/M_V - 1)} \quad (9)$$

with y_z equal to the vapour mole fraction of the low boiling component (R12) at location z. The molar masses of liquid and vapour fractions, M_L and M_V, respectively, are given by

$$M_L = x_z M_1 + (1 - x_z) M_2 \quad (10)$$

Table 2. RMS of CSD equation of state referred to ASHRAE values of saturation pressure, saturated liquid and vapour volume and enthalpy of vaporization for R12 and R114 [9]

	RMS (%)			
Refrigerant	p_{sat}	V_L	V_V	Δi
R12	0.26	0.05	0.29	0.74
R114	0.72	0.34	0.7	2.33

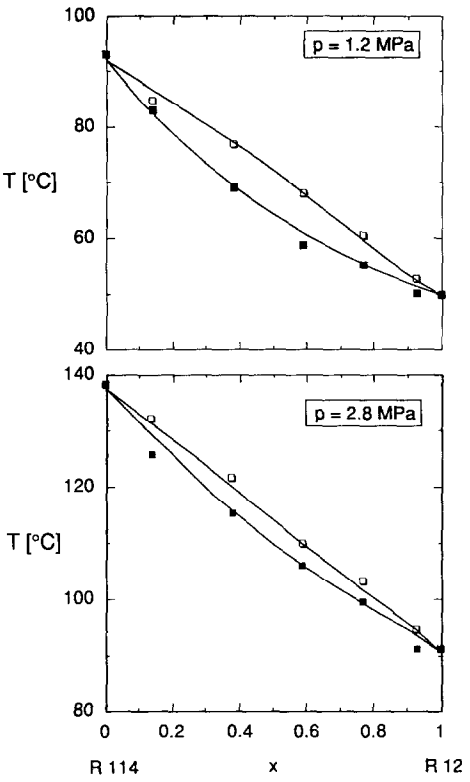

FIG. 4. Temperature–composition diagram of the R12/R114 mixture: comparison of experimental data with the CSD equation of state prediction at 1.2 and 2.8 MPa.

$$M_V = y_z M_1 + (1 - y_z) M_2 \quad (11)$$

with M_1 and M_2 molar masses of R12 and R114, respectively. Equations (7)–(11) have to be solved iteratively together with the CSD equation of state.

EXPERIMENTAL RESULTS

Once the inlet subcooling, the volumetric flow rate and the system pressure are fixed, the test procedure consists of increasing the heat flux up to the occurring of the thermal crisis at the end location $z = 2.1$ m, identified by the sudden increase of the measured wall temperature. The ranges of variation of the parameters in the tests performed were as follows:

		Test matrix
Fluid		R12 (CCl_2F_2), R114 ($C_2Cl_2F_4$)
x_{in}(R12)		0, 0.136, 0.377, 0.586, 0.767, 0.927, 1
p	[MPa]	1.2, 2.8
G	[kg m^{-2} s^{-1}]	400, 800, 1000, 1200, 1400, 1600
$\Delta T_{sub,in}$	[K]	23

Experimental results of mixture CHF are plotted in Fig. 5 as a function of the inlet mole fraction x_{in}(R12),

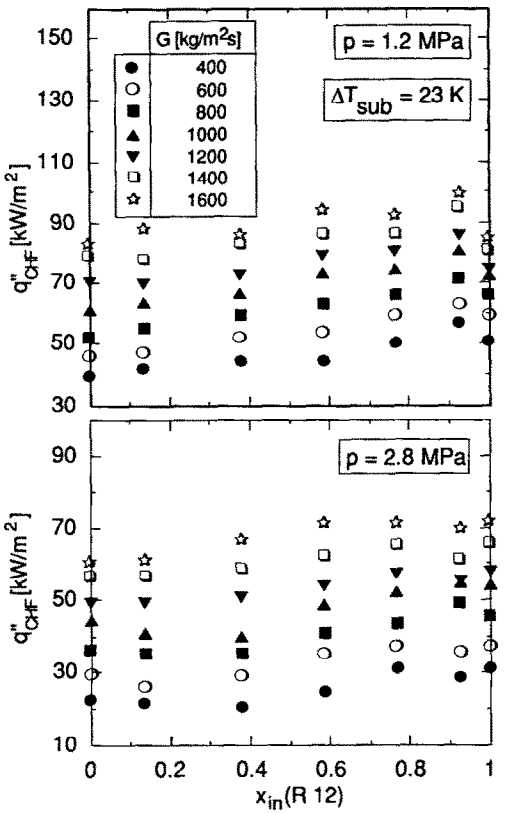

FIG. 5. Experimental CHF of the mixture vs the inlet liquid mole fraction of R12 with mass flux as a parameter.

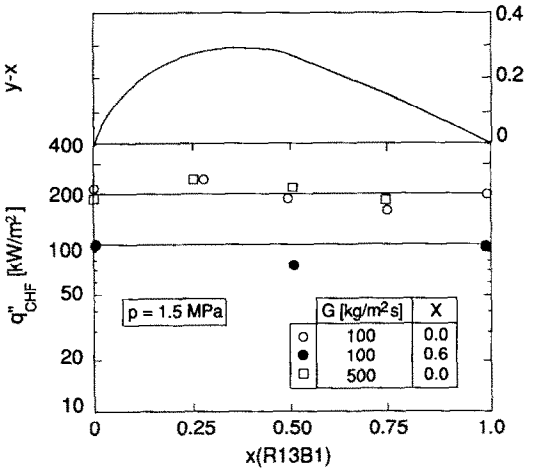

FIG. 6. CHF vs mole fraction of R13B1 at 1.5 MPa (Auracher and Marroquin [8]).

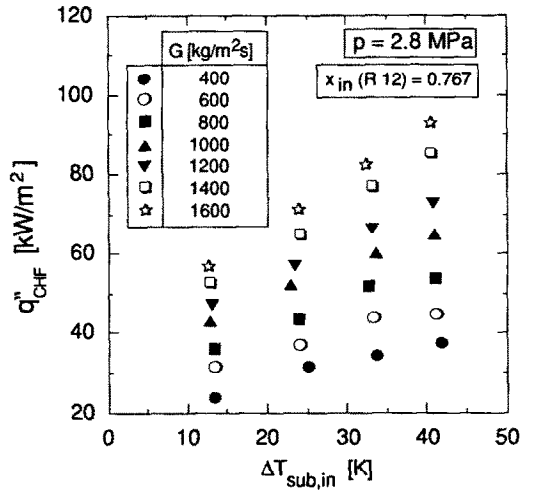

FIG. 7. Experimental CHF vs inlet subcooling at 2.8 MPa for the R12/R114 mixture with $x_{in}(R12) = 0.767$ at various mass fluxes.

with the mass flux as a parameter. The CHF has a similar trend for both the pressures tested. For high reduced pressures, the CHF decreases as pressure increases. At constant pressure, the CHF increases with increasing mass flux and, at constant pressure and mass flux, the CHF is almost linearly dependent on the low boiling fluid mole fraction, x(R12), ranging between those of pure fluids. At the lower pressure tested, the CHF increases linearly with the mole fraction of the more volatile component, x_{in}(R12), and may be represented with the ideal value of CHF for the binary mixtures, evaluated using the linear mole fraction method to correlate the CHF of the two pure components at the same pressure, velocity and subcooling, as:

$$q''_{CHF,i} = [x q''_{CHF,1} + (1-x) q''_{CHF,2}]. \qquad (12)$$

Concerning the 2.8 MPa tests, the trend follows the linear fashion for inlet mole fractions below 0.5, while a constant value for each mass flux is achieved for compositions of the mixture above 50%. Present experimental results are in a good qualitative agreement with Auracher and Marroquin [8] data, obtained using a R13B1/R114 mixture. A typical plot of Auracher and Marroquin's data is shown in Fig. 6, where three different sets of data are reported using the local quality, X, as a parameter. It is interesting to note that the lower CHF corresponding to the higher quality $X = 0.6$ confirms the known effect on CHF due to the inlet subcooling. This effect has also been evaluated in the present study, testing four different values of inlet subcooling, keeping pressure and mole fraction constant, and using the mass flux as a parameter. Experimental results obtained at $p = 2.8$ MPa and $x_{in}(R12) = 0.767$ are shown in Fig. 7, where the CHF is plotted versus the inlet subcooling. As expected, the CHF increases with the inlet subcooling in an almost linear fashion. Moreover, using the method proposed by Auracher and Marroquin [8] to evaluate the local liquid mole fraction of the low boiling fluid, it is possible to link the local quality at the boiling crisis, X_{CHF}, with the actual liquid mixture composition at the CHF quota. This latter is different from the inlet composition, $x_{in}(R12)$ because of the different volatility of the two fluids.

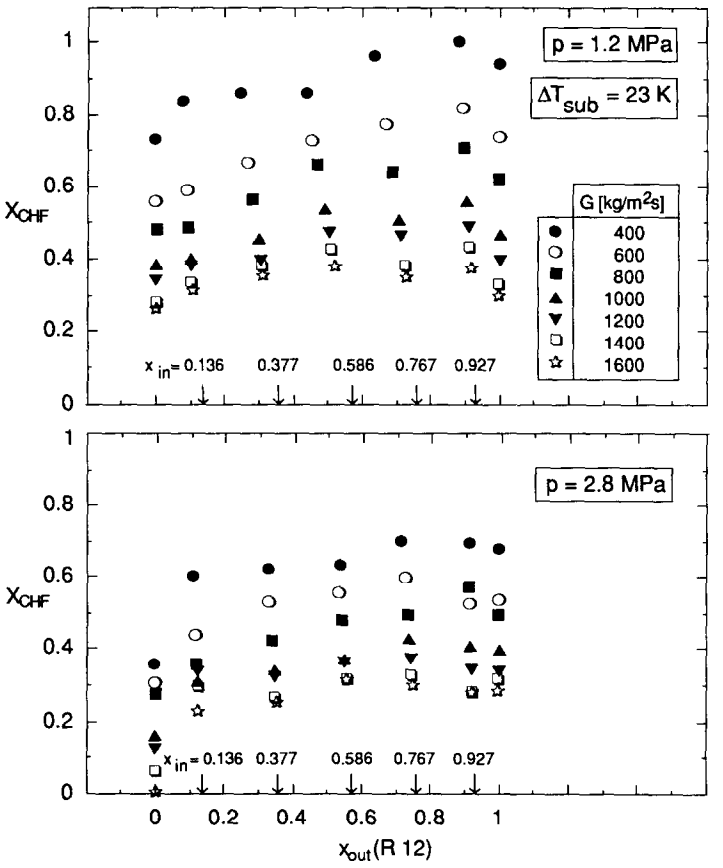

FIG. 8. Local quality at the CHF vs the local liquid mole fraction of R12 at 1.2 and 2.8 MPa using the mass flux as a parameter.

Critical heat flux quality is plotted versus outlet liquid mole fraction of the more volatile component, x_{out}(R12), in Fig. 8, for the two pressures at constant inlet subcooling and using the mass flux as a parameter. The variation of the liquid composition increases as the local quality increases, and decreases with the increasing of mass flux and pressure, even though a stronger effect is observed in the high quality region ($X_{CHF} > 0.5$). Looking at Fig. 8, the variation of the quality at the CHF with the local liquid composition, at constant mass flux, may be deduced. At the low pressure tested and for liquid mixture composition above 50% of R12, the quality tends to be independent of the mixture composition for each mass flux. For the high pressure tests, the quality appears to be decisely independent of the mixture composition for mixture mole fractions above 0.2. The above described trend encourages one to consider that a different mechanism of boiling crisis is present where the local quality at CHF changes with respect to the case when the value of the local quality is constant. As is well known from previous investigations [1–7], particularly that one carried out on burnout by Levitan and Lantsman [16], there are mainly two different mechanisms of thermal crisis: the departure from nucleate boiling (DNB) and the dryout. The first mechanism is associated with the nucleate boiling heat transfer regime and is typical of low quality and high heat flux conditions, and is characterized by a variation of the critical quality with the CHF. The dryout, as verified by Levitan and Lantsman [16], is associated

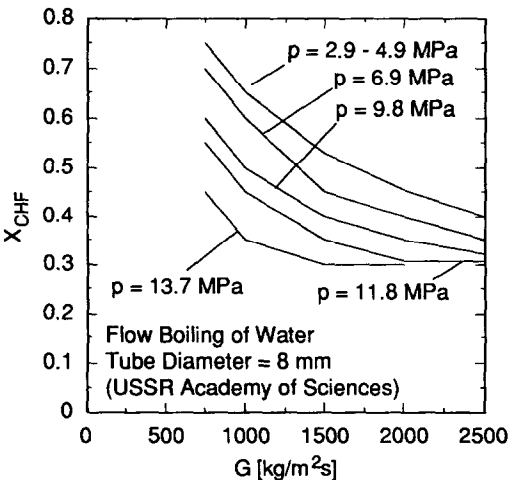

FIG. 9. Dryout curves for water at different pressures (USSR Academy of Sciences [16,17]).

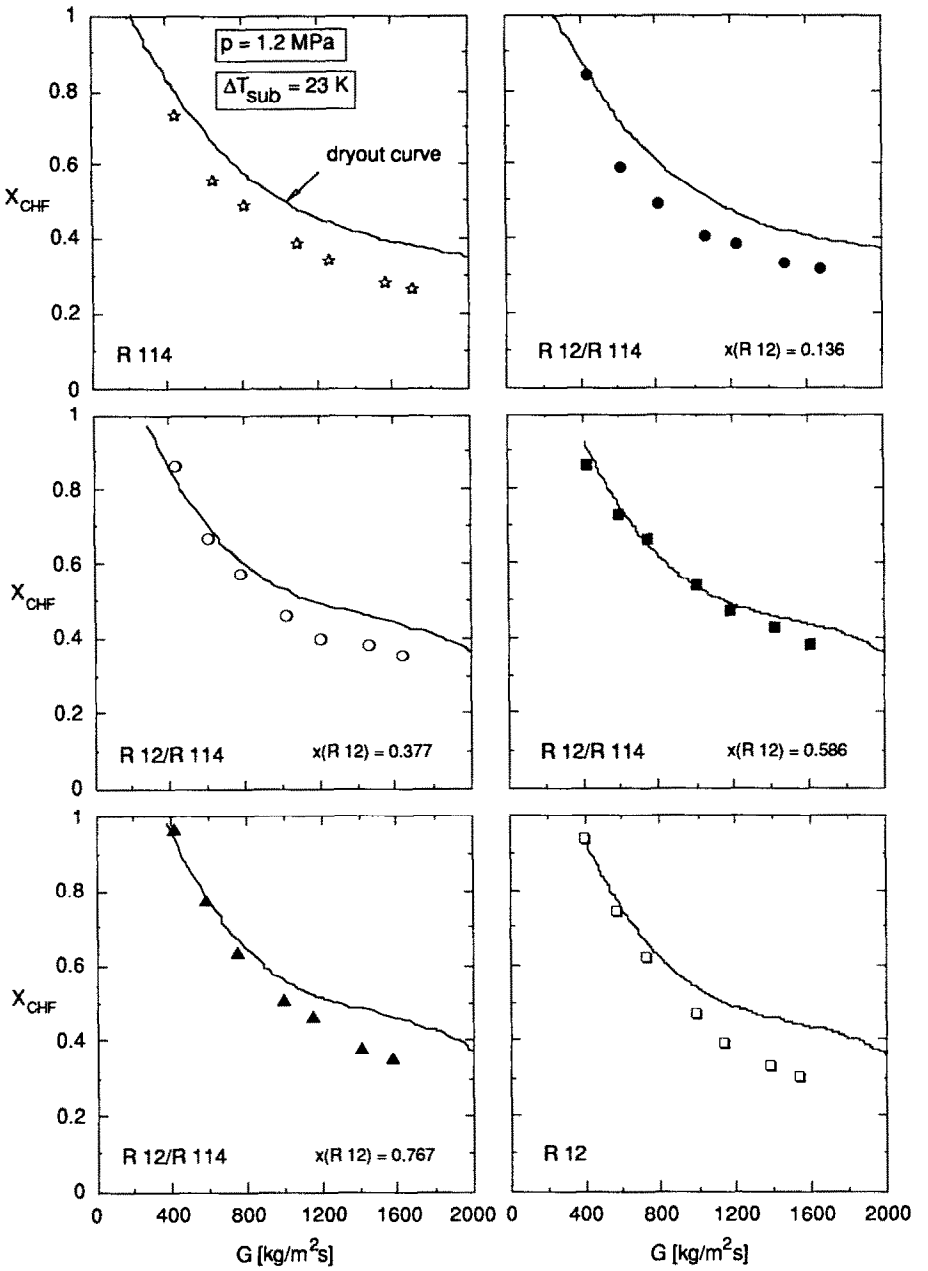

FIG. 10. Comparison of experimental quality at the CHF with the scaled dryout curves [16] at different mixture compositions and pressures.

with the convective boiling regime and is typical of higher qualities and lower heat fluxes, with a limiting value of critical quality essentially independent of the heat flux. Levitan and Lantsman [16] recommended the values of the limiting dryout quality conditions for low heat fluxes, with water as refrigerant, and presented graphically their results for a 8 mm ID tube, as shown in Fig. 9. The burnout data have also been tabulated by the members of the USSR Academy of Sciences [17]. The plot in Fig. 9 clearly indicates that increasing the mass flux decreases the dryout quality. At a lower value of the critical quality, with respect to the dryout curve, the boiling crisis may be thought to be of the DNB type. Starting from the above premises and using the scaling laws proposed by Ahmad [18] to scale the dryout curves for the refrigerants, it is possible to compare present experimental data with the derived dryout curves, as shown in Fig. 10. The experimental data reported in the figure for all the compositions tested have been obtained at the same pressure and inlet subcooling. The pure fluids show different mechanisms of crisis, while the mixtures tend

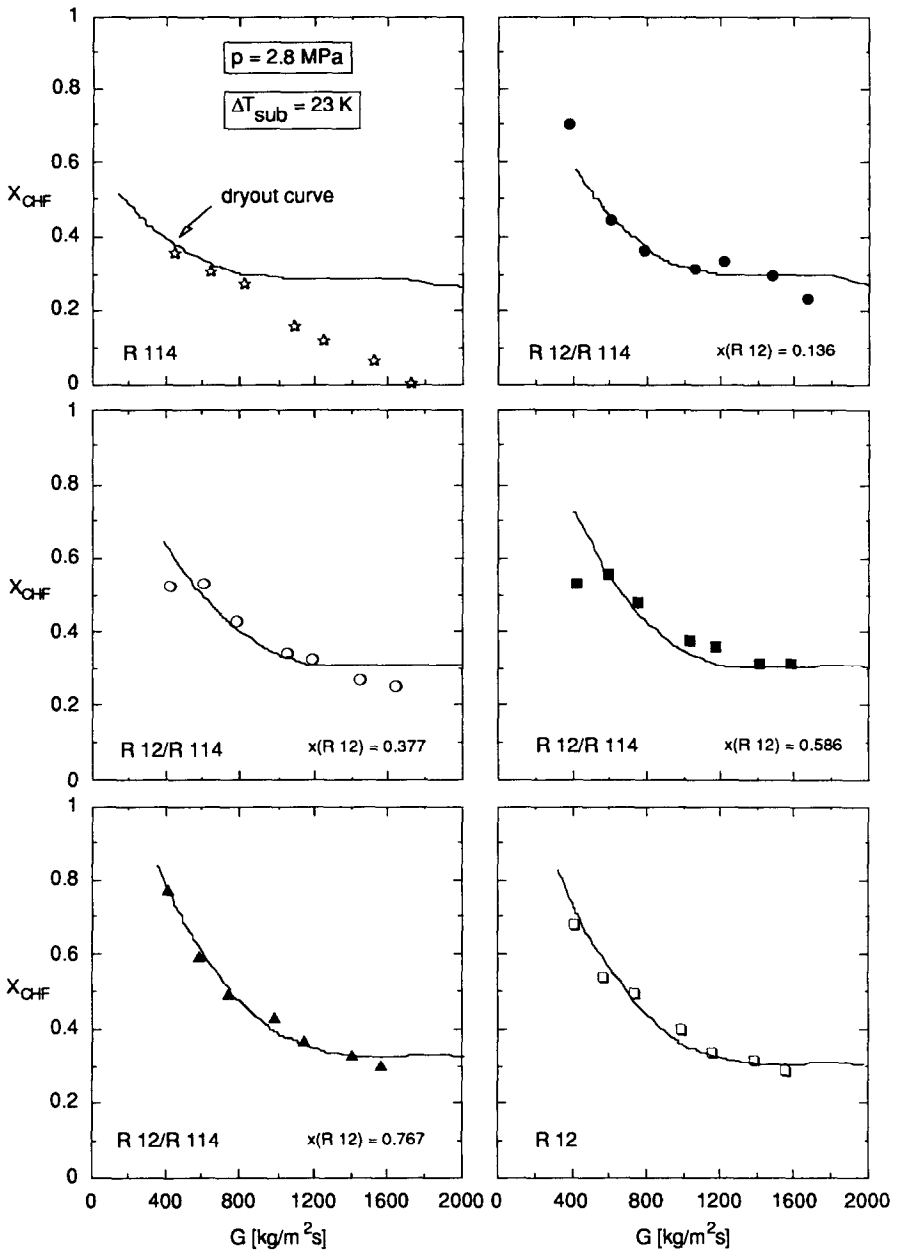

FIG. 10. *Continued.*

to be governed by the mechanism of crisis typical of the more volatile component (R12). In fact, examining the trend of the CHF data of R114 with respect to the dryout curve, only at 2.8 MPa and low mass fluxes (below 1000 kg m^{-2} s^{-1}) the dryout is expected. Looking now at the corresponding R12 tests, most of the points lie on the dryout curve; the corresponding mixture data also tend to lie on the dryout curve. This aspect is connected to the additional limitation in the bubble growth that occurs in a binary liquid mixture as a result of the liquid close to the bubble interface becoming depleted in the more volatile component (R12) (Van Stralen [19]). This aspect sharply reduces the bubble growth rate from that for a single component system, and in particular the vapour produced from the evaporation of the microlayer underneath a bubble will be progressively less rich in the more volatile component (R12) than that produced from the rest of the bubble–liquid interface, as shown in Fig. 11. Thus, the behaviour of the mixture close to the crisis point tends to that of the more volatile component (R12). In conclusion, most of the present experimental data have to be connected with the dryout mechanism of the thermal crisis, with a negligible dependence on the mixture composition, while a linear relationship between the CHF and the mole fraction

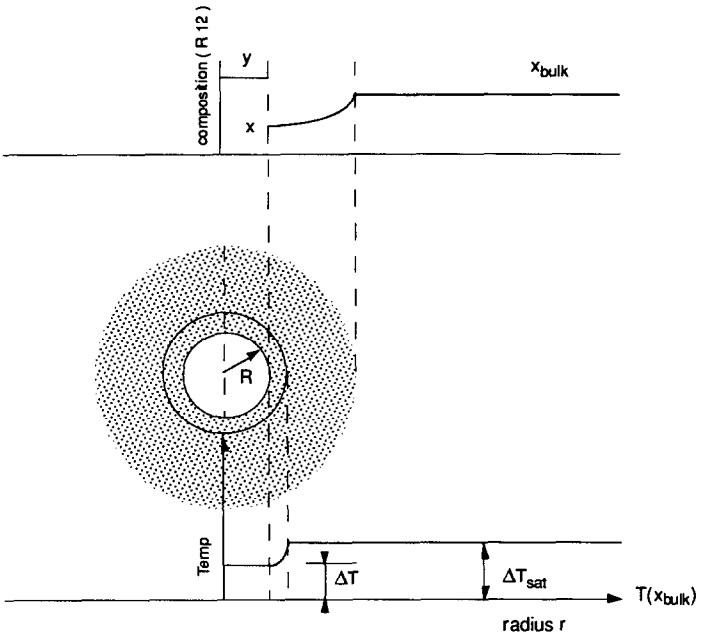

FIG. 11. The growth of a vapour bubble in binary mixtures (Van Stralen [19]).

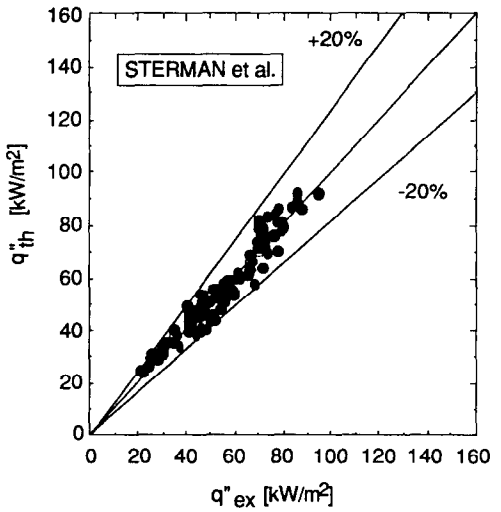

FIG. 12. Comparison of the predicted CHF by Sterman *et al.* correlation [3] with the experimental data.

of the more volatile component (R12) has been verified for the tests connected with the different mechanism of crisis (DNB).

DATA REDUCTION

Most of correlations and models developed to predict the CHF in forced convective boiling are for pure fluids only. As reported by Collier [7], a way of calculating the CHF for binary mixture is to express the CHF value, in analogy with the treatment by Stephan and Körner [20] for pool boiling heat transfer coefficients of mixtures, as a series of two terms: the first term, $q''_{CHF,i}$ is the ideal value of CHF for the binary mixture, evaluated using the linear mole fraction method to correlate the CHF of the two pure components at the same pressure, velocity and subcooling; the second term, $q''_{CHF,E}$, is an additional term connected to the increasing of CHF due to mass transfer effects at the liquid–bubble interface. Thus, the final expression is given by

$$q''_{CHF,mix} = q''_{CHF,i} + q''_{CHF,E} = q''_{CHF,i}(1+\chi) \quad (13)$$

where $q''_{CHF,i}$ has been defined in equation (12).

Sterman *et al.* [3] verified in their experiments that χ varies between 0 and 0.8 and proposed an expression for χ:

$$\chi = K\frac{|y-x|^3}{Re_2} + W\frac{|y-x|^{1.5}}{Re_2^{0.4}}\left[\frac{T_{sat,l}}{T_{sat,mix}-T_{sat,l}}\right] \quad (14)$$

with $K = 3.2\times10^5$; $W = 6.9$.

A comparison of the CHF correlation predicted by the Sterman *et al.* with the experimental results is shown in Fig. 12. The proposed method provides a good evaluation of the experimental values, with all the predictions within the $\pm 20\%$ error band.

A further approach may be followed, considering the almost linear dependence of the CHF on the mixture composition. This simply suggests to employ the pure fluid correlations also in the case of non-azeotropic binary mixtures using the physical properties of the mixture. Among the wide number of correlations, those developed also for refrigerants were chosen, and in particular two of them, the modified CISE correlation [21] and the Katto correlation [22], were

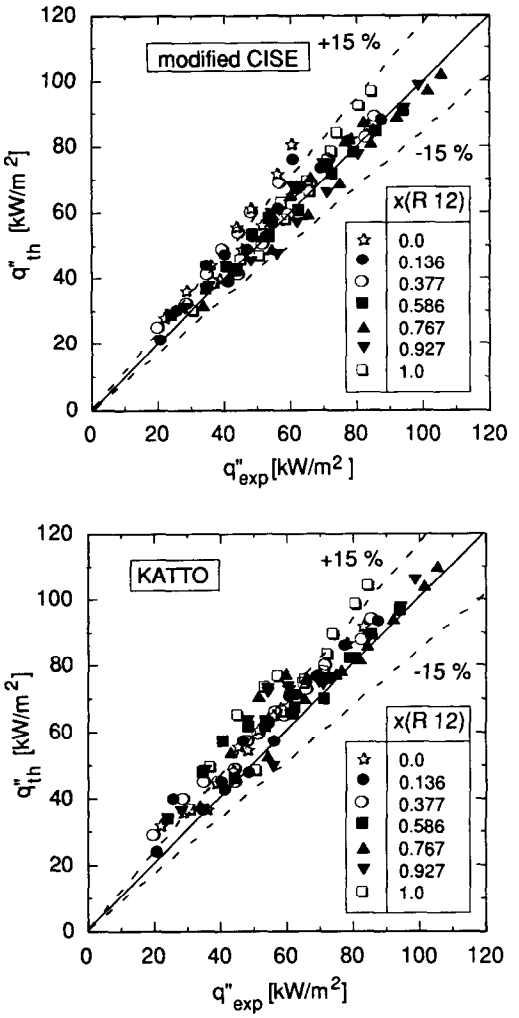

FIG. 13. Comparison of the predicted CHF by modified CISE [21] and Katto [22] correlations with the experimental data.

tested against present data. In applying the two correlations, the inlet conditions have been used. Predicted versus experimental CHF is plotted in Fig. 13 using the inlet mole fraction of the mole volatile component (R12) as a parameter, and with the physical properties evaluated as previously described. The modified CISE correlation shows a better performance than the Katto correlation, that overpredicts the experimental data. The good performance of the modified CISE correlation makes this one very attractive also for its easier applicability, considering the simpler expression with respect to the Katto correlation. Finally, both the Sterman *et al.* and the modified CISE correlations may be successfully used to evaluate the CHF of refrigerant binary mixtures.

CONCLUSIONS

The analysis of the experimental data on binary mixtures R12/R114 in upflow forced boiling shows a different effect of the composition of the mixture on the CHF. In the case of DNB type crisis, a linear dependence on inlet mole fraction of the CHF is observed, while, in the dryout conditions, this dependence becomes negligible. The trend connected with the DNB mechanism of crisis may be well represented with the ideal value of CHF for the binary mixtures.

The comparison of the theoretical CHF, obtained using the correlations by Sterman *et al.*, modified CISE and Katto, with the experimental data shows a good performance of the first two correlations, while a systematic overprediction is provided by the Katto correlation.

Acknowledgements—The authors are deeply indebted to G. Farina, who performed the experimental runs. Thanks are also due to A. M. Moroni, for the editing of the article.

REFERENCES

1. V. I. Tolubinsky and P. S. Matorin, Forced convection boiling heat transfer crisis with binary mixtures, *Heat Transfer—Sov. Res.* **5**(2), 98–101 (1973).
2. D. G. Andrews, F. C. Hooper and P. Butt, Velocity, subcooling and surface effects in the departure from nucleate boiling of organic binaries, *Can. J. Chem. Engng* **46**, 194–199 (1968).
3. L. Sterman, A. Abramov and G. Checheta, Investigation of boiling crisis at forced motion of high temperature organic heat carriers and mixtures, *Int. Symposium on Research into Co-current Gas–Liquid Flow, Univ. of Waterloo, Ontario, Canada*, Paper E2, 1968
4. K. V. Naboichenko, A. A. Kiryutin and B. S. Gribov, A study of critical heat flux with forced flow of monoisopropyldiphenyl–benzene mixture, *Teploenergetika* **12**(11), 81–86 (1965).
5. M. Carne, Studies of the critical heat flux for some binary mixtures and their components, *Can. J. Chem. Engng* **42**, 235–240 (1963).
6. A. E. Bergles and L. S. Scarola, Effect of a volatile additive on the critical heat flux for surface boiling of water in tubes, *Chem. Engng Sci.* **21**, 721–723 (1966).
7. J. G. Collier, *Convective Boiling and Condensation* (2nd Edn), pp. 394–426. McGraw-Hill, New York (1981).
8. H. Auracher and A. Marroquin, Forced convection critical heat flux and transition boiling of mixtures flowing upward in a vertical tube, *European Two-Phase Flow Group Meeting*, Paper B1, Stockholm, 1–3 June (1992).
9. G. Morrison and M. McLinden, Application of a hard sphere equation of state to refrigerants and refrigerant mixtures, NBS Technical Note 1226, NBS, Gaithersburg, Maryland (1986).
10. *ASHRAE Handbook of Fundamentals*. American Society of Heating, Refrigerant and Air Conditioning Engineer, Inc., New York (1981).
11. L. P. Filippov, *Vest. Mosk. Univ., Ser. Fiz. Mat. Estestv. Nauk.* **8**, 67–69 (1955).
12. S. G. Kandlikar, C. A. Bijlani and S. P. Sukhatme, Predicting the properties of mixtures of R22 and R12—Part II. Transport properties, *ASHRAE Trans. No.* 2343 (1975).
13. C. R. Wilke, A viscosity equation for gas mixtures, *J. Chem. Phys.* **18**, 517–519 (1950).
14. D. S. Jung and R. Radermacher, Prediction of pressure drop during horizontal annular flow boiling of pure and mixed refrigerants, *Int. J. Heat Mass Transfer* **32**, 2435–2446 (1989).
15. M. Niederkrüger, Strömungssieden von reinen Stoffen

und binären zeotropen Gemischen im waagerechten Rohr bei mittleren und hohen Drücken, Fortschritt-Berichte VDI, Reihe 3, No. 245, VDI-Verlag (1991).
16. L. L. Levitan and F. P. Lantsman, Investigating burnout with flow of steam–water mixture in a round tube, *Teploenergetika* **22**(1), 80–83 (1975).
17. USSR Academy of Sciences, Tabular data for calculating burnout when boiling water in uniformly heated round tubes, *Teploenergetika* **23**(9), 90–92 (1976).
18. S. Y. Ahmad, Fluid to fluid modelling of critical heat flux: a compensated distortion model, *Int. J. Heat Mass Transfer* **16**, 641–661 (1973).
19. S. T. D. Van Stralen, Bubble growth rates in boiling binary mixtures, *Brit. Chem. Engng* **12**(3), 390–394 (1967).
20. K. Stephan and M. Körner, Calculation of heat transfer in evaporating binary liquid mixtures, *Chemie-Ingr-Tech.* **41**, 409–417 (1969).
21. G. P. Celata, M. Cumo, F. D'Annibale, G. E. Farello and T. Setaro, Flow transient experiments with Refrigerant-12, *Revue Generale de Thermique* **XXV**(299), 513–519 (1986).
22. Y. Katto and H. Ohno, An improved version of the generalized correlation of critical heat flux for the forced convective boiling in uniformly heated vertical tubes, *Int. J. Heat Mass Transfer* **27**, 1641–1648 (1984).